Supplemental Information

DLK1/*DIO3* locus upregulation

by a β-catenin-dependent enhancer drives cell

proliferation and liver tumorigenesis

Julie Sanceau, Lucie Poupel, Camille Joubel, Isabelle Lagoutte, Stefano Caruso, Sandra Pinto, Christèle Desbois-Mouthon, Cécile Godard, Akila Hamimi, Enzo Montmory, Cécile Dulary, Sophie Chantalat, Amélie Roehrig, Kevin Muret, Benjamin Saint-Pierre, Jean-François Deleuze, Sophie Mouillet-Richard, Thierry Forné, Christophe F. Grosset, Jessica Zucman-Rossi, Sabine Colnot, and Angélique Gougelet

Supplemental material

Table S1: Top 20 overexpressed RNAs in Apc$^{\Delta hep}$ *versus* wild-type or βcatenin$^{\Delta hep}$ hepatocytes from RNAseq data. Results are represented as the log2 fold induction in Apc$^{\Delta hep}$ *versus* wt hepatocytes (second column) and versus β-catenin$^{\Delta hep}$ (βcat$^{\Delta hep}$) hepatocytes (fourth column) with their respective pvalue (pval). RNAs produced from the *Dlk1/Dio3* locus are indicated in bold and grey.

gene	Log2 Apc$^{\Delta hep}$ / wt	pval	Log2 Apc$^{\Delta hep}$/βcat$^{\Delta hep}$	pval
Eln	10.6	5.9E-42	20.0	1.0E-50
Wisp2	9.3	1.0E-50	10.8	1.0E-50
Akr1c18	7.8	4.0E-16	7.7	2.8E-23
Rian	**7.6**	**1.0E-50**	**20.0**	**1.0E-50**
Nkd1	7.5	1.0E-50	7.4	1.0E-50
AK133155	7.3	1.1E-27	7.8	1.0E-43
Slpi	7.1	1.0E-50	7.2	1.0E-50
Rtl1	**6.8**	**7.1E-10**	**20.0**	**4.4E-15**
Akr1b7	6.6	1.0E-50	8.4	1.0E-50
Meg3	**6.5**	**1.0E-50**	**13.5**	**1.0E-50**
Pkp1	6.5	7.0E-13	20.0	7.4E-21
Prom1	6.5	2.1E-13	5.9	2.1E-18
Prr18	6.4	7.3E-13	20.0	9.6E-21
Kif26b	6.2	5.3E-38	9.7	1.0E-50
Trib2	6.1	4.0E-31	6.7	1.0E-50
BC023483	6.1	4.3E-02	5.0	4.2E-02
Mirg	**6.1**	**4.5E-26**	**20.0**	**1.0E-50**
Reep1	6.1	1.7E-14	6.7	4.6E-22
Ihh	6.1	6.5E-30	9.2	1.0E-50
Elovl7	5.9	3.2E-06	20.0	1.5E-09

Table S2: Top 20 overexpressed miRNAs in Apc$^{\Delta hep}$ *versus* wt hepatocytes from small-RNAseq data. Results are represented as the log2 fold induction in Apc$^{\Delta hep}$ *versus* wt hepatocytes (second column) or versus βcat$^{\Delta hep}$ (fourth column) with their respective adjusted pvalue (padj). MiRNAs produced from the *Dlk1/Dio3* locus are indicated in bold and grey.

miRNA	Log2 Apc$^{\Delta hep}$ / wt	padj	Log2 Apc$^{\Delta hep}$/bcat$^{\Delta hep}$	padj
mmu-miR-341	6.7	4.3E-31	7.0	1.8E-60
mmu-miR-665	6.7	4.5E-26	8.7	1.9E-53
mmu-miR-136	6.7	1.8E-69	8.2	2.2E-140
mmu-miR-433	6.4	1.7E-17	7.5	1.5E-29
mmu-miR-377	5.9	6.5E-07	10.0	2.0E-09
mmu-miR-329	5.9	2.7E-07	5.0	7.6E-08
mmu-miR-127	5.9	2.9E-51	7.7	6.3E-130
mmu-miR-431	5.8	3.6E-22	7.4	2.0E-47
mmu-miR-370	5.7	4.4E-18	7.4	1.5E-35
mmu-miR-487b	5.4	8.2E-11	5.5	1.7E-15
mmu-miR-434-3p	5.4	4.3E-31	7.7	4.3E-92
mmu-miR-496	5.4	6.1E-08	6.4	6.3E-11
mmu-miR-381	5.4	1.1E-26	6.5	6.5E-65
mmu-miR-434-5p	5.3	1.3E-29	7.7	4.9E-90
mmu-miR-543	5.2	6.7E-13	10.0	1.1E-25
mmu-miR-376a	5.2	1.3E-17	5.9	1.3E-35
mmu-miR-376b	5.2	2.9E-21	6.5	1.7E-50
mmu-miR-134	5.2	3.4E-32	6.0	5.1E-77
mmu-miR-495	5.1	1.2E-11	5.1	1.0E-17
mmu-miR-409-3p	5.0	1.4E-26	6.4	1.3E-71

Table S3: pathological and molecular characteristics of the pediatric cohort 1

Patient	Samples	Gender	Age (months)	TV	VI	S/MN	M	SC	CH	P	CHIC-HS	Risk	AFP (ng/mL)	ß-catenin RNAseq
P02	T/NT	F	11	60	N	S	N	N	Y	II	B	SR	153840	exon3 del
P04_a	T/NT	F	14	197	N	S	N	N	N	II	B	SR	300	exon3 del
P04_c	T/NT	F	14	197	N	S	N	N	Y	II	B	SR	300	exon3 del
P09	T	F	6	160	N	S	N	N	Y	III	B	NA	401807	exon3 del
P15	T/NT	M	5	760	N	S	N	N	Y	II	B	SR	56613	exon3 del
P16	T/NT	M	36	800; 500	Y	M	N	N	Y	IV	D	HR	54982	WT
P17	T/NT	M	12	520	N	S	N	Y	Y	II	B	SR	837000	exon3 del
P19	T/NT	M	9	2	N	S	N	Y	Y	I	B	HR	88000	in frame deletion aa15-
P20	T/NT	F	12	41	N	S	N	N	Y	II	B	SR	318800	D32V
P22	NT	F	NA	2	Y	M	Y	Y	Y	III	D	HR	2000000	G34V
P23	T/NT	M	50	4	Y	M	Y	Y	Y	II	D	HR	350000	in frame deletion aa25-
P24	T/NT	M	4	5	N	M	N	Y	Y	III	C	SR	82000	S37A
P26_b	T/NT	M	28	2 805	Y	M	Y	Y	Y	II	D	HR	1500000	in frame deletion aa37-
P27	T/NT	F	NA	598	N	S	N	N	Y	II	B	SR	2355000	G34V
P28	T/NT	F	11	1 540	Y	M	N	Y	Y	IV	C	HR	360000	exon3 del
P29	T/NT	F	NA	NA	N	S	N	N	N	II	A	NA	300	in frame deletion aa19-
P32	T/NT	F	4	1	N	S	N	N	Y	II	B	SR	934371	WT
P33	T/NT	M	10	241	N	M	N	Y	Y	III	C	SR	300000-500000	in frame deletion aa28-
P34	T	M	4	520	N	S	N	N	Y	III	B	SR	518000	T41A
P35	T/NT	F	24	912	Y	M	N	Y	Y	II	C	HR	1000000	G34E
P36	T/NT	M	130	NA	N	S	N	N	Y	IV	D	HR	NA	WT
P38	T/NT	M	11	1 584	N	S	N	N	Y	II	B	NA	155385	exon3 del

CH: chemotherapy   SC: Small Cells presence

HR: high risk   S/MN: solitary/multiple nodules

NA: non available   SR: standard risk

M: metastasis   TV: Tumor volume (cm^3)

P: PRETEXT stage   VI: vascular invasion

Children's Hepatic Tumors International Collaboration-Hepatoblastoma Stratification

Table S4: Clinical, pathological and molecular characteristics of the pediatric cohort 2 (n=110) from previously published series [1]

Variable		Total (%)
Age (months)	[median. min-max]	33 (3-278)
Gender	Male : Female	65 (59%) : 45 (41%)
Sample Type	Primary hepatoblastoma	83 (75%)
	Hepatoblastoma relapse	3 (3%)
	Hepatoblastoma metastasis	14 (13%)
	Hepatocellular carcinoma	10 (9%)
Etiology	Without known etiology	94 (85%)
	Other*	16 (15%)
Chemotherapy	yes	84 (76%)
	no	26 (24%)
Transcriptomic group	Hepatocyte 1	21 (25%)
	Hepatocyte 2	19 (23%)
	Liver Progenitor	33 (40%)
	Mesenchymal	10 (12%)
CTNNB1 **mutations**	Mutated	92 (92%)
	Non-mutated	8 (8%)

*Beckwith Wiedmann Syndrome; Familial Adenomatous Polyposis; Mitochondrial Cytopathy. Progressive familial intrahepatic cholestasis. Tyrosinemia. Simpson Golabi Behmel Syndrome.

Table S5: Top 20 under-expressed RNAs in Apc$^{\Delta hep}$-DLK1/DIO3$^{\Delta WRE}$ *versus* Apc$^{\Delta hep}$-Rosa26 hepatocytes from RNAseq data. Results are represented as the log2 fold induction in Apc$^{\Delta hep}$-DLK1/DIO3$^{\Delta WRE}$ *versus* Apc$^{\Delta hep}$-Rosa26 hepatocytes and their respective adjusted p-value (padj). RNAs produced from the *Dlk1/Dio3* locus are indicated in bold and grey.

gene	Log2 Apc$^{\Delta hep}$ DLK1/DIO3$^{\Delta WRE}$/ Apc$^{\Delta hep}$ Rosa26	p-adj
Oxtr	-5.12	2.0E-03
Gm37899	**-2.81**	**9.0E-03**
Gm27000	-2.81	2.0E-03
B830012L14Rik	**-2.65**	**1.0E-02**
Hba-a1	-2.63	4.0E-02
Drp2	-2.61	1.0E-02
Mirg	**-2.49**	**3.5E-08**
Rtl1	**-2.47**	**4.5E-07**
Rian	**-2.29**	**2.4E-16**
Gm12248	-2.05	2.0E-02
Meg3	**-2.03**	**6.0E-03**
Depdc1a	-1.9	4.0E-03
Col6a3	-1.75	5.0E-03
Gm48302	-1.75	3.0E-02
Cenpf	-1.7	3.0E-02
Cip2a	-1.69	3.0E-05
Melk	-1.69	8.0E-03
Nuf2	-1.61	2.0E-03
Kif20b	-1.61	3.0E-03
Pla2r1	-1.58	2.0E-04

Table S6: Top 20 under-expressed miRNAs in Apc$^{\Delta hep}$-DLK1/DIO3$^{\Delta WRE}$ _versus_ Apc$^{\Delta hep}$-Rosa26 hepatocytes from small RNAseq data. Results are represented as the log2 fold induction in Apc$^{\Delta hep}$-DLK1/DIO3$^{\Delta WRE}$ _versus_ Apc$^{\Delta hep}$-Rosa26 hepatocytes and their respective adjusted p-value (padj). miRNAs produced from the _Dlk1/Dio3_ locus are indicated in bold.

miRNA	Log2 Apc$^{\Delta hep}$ DLK1/DIO3$^{\Delta WRE}$ / Apc$^{\Delta hep}$ Rosa26	p-adj
mmu-miR-337-5p	0.47	2.3E-05
mmu-miR-127-3p	0.47	2.9E-05
mmu-miR-154-5p	0.47	1.4E-04
mmu-miR-299a-3p	0.48	8.4E-04
mmu-miR-543-3p	0.48	1.1E-03
mmu-miR-134-5p	0.51	9.1E-05
mmu-miR-496a-3p	0.52	6.1E-03
mmu-miR-154-3p	0.52	8.6E-03
mmu-miR-409-3p	0.53	2.6E-04
mmu-miR-434-5p	0.54	2.7E-03
mmu-miR-379-3p	0.54	4.5E-03
mmu-miR-376b-3p	0.54	6.2E-03
mmu-miR-434-3p	0.56	5.8E-04
mmu-miR-1193-3p	0.56	5.0E-03
mmu-miR-494-3p	0.57	3.7E-03
mmu-miR-299b-3p	0.57	1.4E-02
mmu-miR-376a-3p	0.57	1.7E-02
mmu-miR-136-5p	0.57	2.5E-02
mmu-miR-337-3p	0.57	3.5E-02
mmu-miR-376a-5p	0.57	3.6E-02

Table S7: Most significantly under-expressed RNAs in Apc$^{\Delta hep}$-DLK1/DIO3$^{\Delta WRE}$ *versus* Apc$^{\Delta hep}$-Rosa26 hepatocytes from RNAseq data. Results are represented as the log2 fold induction in Apc$^{\Delta hep}$-DLK1/DIO3$^{\Delta WRE}$ *versus* Apc$^{\Delta hep}$-Rosa26 hepatocytes and their respective adjusted p-value (padj). RNAs produced from the *Dlk1/Dio3* locus are indicated in bold and grey and those involved in cell cycle process in red.

gene	Log2 Apc$^{\Delta hep}$ DLK1/DIO3$^{\Delta WRE}$ / Apc$^{\Delta hep}$ Rosa26	p-adj
Rian	**-2.29**	**2.4E-16**
Mirg	**-2.49**	**3.5E-08**
Rtl1	**-2.47**	**4.5E-07**
Kif20a	-1.36	3.0E-06
Cip2a	-1.69	3.0E-05
Pla2r1	-1.58	2.0E-04
Ifi213	-1.12	2.0E-03
Gm27000	-2.81	2.0E-03
Nuf2	-1.61	2.0E-03
Ccnb1	-1.22	2.0E-03
Ckap2	-1.52	2.0E-03
Oxtr	-5.12	2.0E-03
Top2a	-0.99	2.0E-03
Thrsp	-1.03	2.0E-03
Kif4	-0.99	2.0E-03
Nedd4l	0.62	3.0E-03
Kif20b	-1.61	3.0E-03
Ccna2	-1.04	3.0E-03
Depdc1a	-1.9	4.0E-03
Hmmr	-1.27	4.0E-03
Nusap1	-1.22	4.0E-03
Slc25a30	1.42	5.0E-03
Rbpms	0.89	5.0E-03
Mndal	-0.97	5.0E-03
Col6a3	-1.75	5.0E-03
Meg3	**-2.03**	**6.0E-03**
Melk	-1.69	8.0E-03
Gm37899	**-2.81**	**9.0E-03**
Racgap1	-0.95	1.0E-02
Drp2	-2.61	1.0E-02
Pdilt	-0.70	1.0E-02
Atp8a1	-1.08	1.0E-02
Mir99ahg	-1.55	1.0E-02
B830012L14Rik	**-2.65**	**1.0E-02**
Slc34a2	-1.12	2.0E-02
Gm12248	-2.05	2.0E-02
Foxa2	0.82	2.0E-02
Rnf144a	1.27	2.0E-02
Cdca3	-0.82	2.0E-02
Mgat4b	0.72	2.0E-02
Flot1	0.60	2.0E-02
Chic1	-0.80	2.0E-02
Slc33a1	-0.48	2.0E-02
Gm48302	-1.75	3.0E-02
Insig1	-0.75	3.0E-02

Foxa3	0.45	3.0E-02
Cenpf	-1.7	3.0E-02
Zxda	1.24	3.0E-02
mt-Atp6	-0.75	3.0E-02
Cdk1	-0.76	4.0E-02
Hba-a1	-2.63	4.0E-02
Gas2l3	-0.98	4.0E-02
Rasa2	1.16	4.0E-02
Gm32540	2.45	4.0E-02
Hmga1b	4.97	4.0E-02
Rab35	0.57	4.0E-02
Ncapg2	-1.23	5.0E-02

Table S8: RNAseq data for regulators of cell cycle progression and cytokinesis. Results are represented as the log2 fold induction in Apc$^{\Delta hep}$ *versus* wild-type hepatocytes and Apc$^{\Delta hep}$-DLK1/DIO3$^{\Delta WRE}$ *versus* Apc$^{\Delta hep}$-Rosa26 hepatocytes and their respective adjusted p-value (padj); in green: down-regulation. in orange: up-regulation.

gene	Log2 Apc$^{\Delta hep}$ vs wt	pvalue	Log 2 Apc$^{\Delta hep}$ DLK1/DIO3$^{\Delta WRE}$ vs Apc$^{\Delta hep}$	padj
Kif4	2.7	1E-05	-1.0	2E-03
Kif20a	2.4	1E-10	-1.4	3E-06
Kif20b	3.9	1E-06	-1.6	2E-03
Nuf2	3.1	4E-05	-1.6	3E-03
Nusap1	2.8	4E-05	-1.2	4E-03
Top2a	2.8	3E-12	-1.0	2E-03
Gas2l3	1.4	1E-02	-1.0	4E-02
Cenpf	2.9	8E-10	-1.7	3E-02
Ckap2	3.1	3E-08	-1.5	2E-03
Depdc1a	2.2	1E-02	-1.9	4E-03
Hmmr	2.1	2E-05	-1.3	4E-03
Racgap1	2.8	1E-07	-1.0	1E-02
Pla2r1	3.1	2E-03	-1.6	2E-04
Rasa2	1.3	6E-02	1.1	4E-02
Flot1	1.0	2E-03	0.6	2E-02
Ccna2	2.3	6E-07	-1.2	2E-03
Ccnb1	2.3	4E-03	-1.2	2E-03
Cdk1	2.6	1E-07	-0.7	4E-02

Table S9: lists of primers and probes used

Name	Sequence	Supplier
Ctnnb1-I2-3	5'-TCAGTATGAGCTCCATGGGAC AGGGGT-3'	Eurogentec[1]
Ctnnb1-I3-1	5'-GACAGCTCAGCCACAGCACAA GTGGGT-3'	Eurogentec[1]
Rosa-1	5'-CTCGATGGAAAATACTCCGAG GCGGAT-3'	Eurogentec[1]
sg2 DLK1-WRE (mouse)	5'- TTCCTCAGTGGGGCTAAAGGA GAGGGT -3'	Eurogentec[1]
Sg5 DLK1-WRE (mouse)	5'- GGATGACCTTTGACTTCTGAA GGGAGT -3'	Eurogentec[1]
Sg1 DLK1-WRE (human)	5'- TATTCAGAGCAAGCCTGTGGC ATGAAT -3'	Eurogentec[1]
Sg2 DLK1-WRE (human)	5'- TACCCTTTAGGTGTTTGCGGA AAGGAT -3'	Eurogentec[1]
Sg3 DLK1-WRE (human)	5'- GCAGGACCCTTCTCAAAGGGC CAGGGT -3'	Eurogentec[1]
Sg3 DLK1-WRE (human)	5'- CTTTGCAGTCGTGAACTGTGG GGGGAT -3'	Eurogentec[1]
Rosa26 editing	F 5'-CTTGCTCTCCCAAAGTCGCT-3' R 5'-CCAATGCTCTGTCTAGGGGT-3'	Eurogentec[1]
Ctnnb1 editing	F 5'-TTTTGGTGTCGGGGCACATA-3' R 5'-CATGGTGCGTACAATGGCAG-3'	Eurogentec[1]
DLK1-WRE editing (mouse)	F 5'-AGCATGGCCGAGTACTCATT-3' R 5'-CCTCTGCATGACCTGTGACT-3'	Eurogentec[1]
DLK1-WRE editing (human)	F 5'-TGAGGCTGCAATGAACCATG-3' R 5'-GGCTTATGTTGTGCAAACGC-3'	Eurogentec[1]
18S	F 5'-GTAACCCGTTGAACCCCATT-3' R 5'-CCATCCAATCGGTAGTAGCG -3'	Eurogentec[1]
Mirg	F 5'-A GCCATCTACCTCTGAGTCCC-3' R 5'-AGAGCAGAAACCCCTCCTTC-3'	Eurogentec[1]
Rian	F 5'-CCAGGTTCAAGGTCCCTCAT-3' R 5'-TCTTGTGTCTCGAAGGCCTT-3'	Eurogentec[1]
Mki67	F 5'-CTGCCTGCGAAGAGAGCATC-3' R 5'-AGCTCCACTTCGCCTTTTGG-3'	Eurogentec[1]
Kif20a	F 5'-AAGTGGTGAGCGGCTAAAGGAG-3' R 5'-GAAGCCTTGGAACACACGAGTC-3'	Eurogentec[1]
Kif20b	F 5'-GGATGACCTAGACGTGCTTACC-3' R 5'-TCGCTTGAGTGGTAAGGACAGC-3'	Eurogentec[1]
Nuf2	F 5'-CCTCTATGGTCAGAATGCAGCAG-3' R 5'-ACTGCTTGAACTCCTCTCGCTC-3'	Eurogentec[1]
Nusap1	F 5'-TTCCTCCAAGAGGAAGGCTCTC-3' R 5'-GGTGTCTTGGTCAGTGAGCACT-3'	Eurogentec[1]
Top2a	F 5'-CAAGCGAGAAGTGAAGGTTGCC-3' R 5'-GCTACCCACAAAATTCTGCGCC-3'	Eurogentec[1]
Cenpf	F 5'- GCACGACTTCAGTTACAGGAGC -3' R 5'- TGCTTTGGTGTTTTCTCTGTAGTC -3'	Eurogentec[1]
Ckap2	F 5'- TACTGACCAGCGCAGATACACG -3' R 5'- TCCTTTGCCAGTTCTCCACTCC-3'	Eurogentec[1]
Ccna2	F 5'- GCCTTCACCATTCATGTGGAT -3' R 5'- TTGCTCCGGGTAAAGAGACAG-3'	Eurogentec[1]
Fadd	F 5'-CACACAATGTCAAATGCCACCTG-3' R 5'-TGCGCCGACACGATCTACTGC-3'	Eurogentec[1]
Ccl2	F 5'-TCTGGGCCTGCTGTTCACA-3' R 5'-GGATCATCTTGCTGGTGAATGA-3'	Eurogentec[1]
Ccl5	F 5'-GCTGCTTTGCCTACCTCTCC-3' R 5'-TCGAGTGACAAACACGACTGC-3'	Eurogentec[1]
Csf1	F 5'-TACAAGTGGAAGTGGAGGAGCCAT-3' R 5'-AGTCCTGTGTGCCCAGCATAGAAT- 3'	Eurogentec[1]
Human FADD	F 5'-ATTAATGCCTCTCCCGCACC-3' R 5'-TCTCTGCTTCGCTCCGATTC-3'	Eurogentec[1]
DLK1-WRE (ChIP)	F 5'-CCTCTTCCTGCCCCTAACGTA-3' R 5'-CCTGTGTCTGGATGACCTTTGA -3'	Eurogentec[1]
Myc-10kb (ChIP control)	F 5'- ACACACCTTGAATCCCGT -3'	Eurogentec[1]

	R 5'- CCCAGCTAGAATGAACAAG -3'	
Kif20a (ChIP)	F 5'- GGT-AAC-CCG-GAC-CCA-CAT-TA -3' R 5'- TGA-TCC-CAG-CTT-CTA-CCC-AC -3'	Eurogentec[1]
Ccna2 (ChIP)	F 5'- CTT-TCT-CTG-TGA-TGC-TGC-CA -3' R 5'- GGG-GTG-GGG-TAG-TTT-ACT-GG -3'	Eurogentec[1]
Cdc2 (ChIP)	F 5'- CGA-GTG-CCA-GCA-GTT-TCA-AA -3' R 5'- GAG-CTC-AAG-AGT-CAG-TTG-GC -3'	Eurogentec[1]
Cenpf (ChIP)	F 5'- ACGAGCGATTCAAACTGCC -3' R 5'- CCAAAAGGGCCAATCAGAGG -3'	Eurogentec[1]
Ig-DMR (ChIP)	F 5'-GACACCCTGCCTTCTCTCTT-3' R 5'-TTCCCTACTGCCCTTCCTTG-3'	Eurogentec[1]
human CCNA2 (ChIP)	F 5'-AGTTCAAGTATCCCGCGACT-3' R 5'-CCCAGCCAGTTTGTTTCTCC-3'	Eurogentec[1]
human KIF20A (ChIP)	F 5'-GGTAACCCGGACCCACATTA-3' R 5'-TTACTCACACCTAGTCGCCG-3'	Eurogentec[1]
human CDC2 (ChIP)	F 5'-TGCTCCGCTGACTAGAAAC-3' R 5'-GTTTCAAACTCACCGCGCTA-3'	Eurogentec[1]
F1 (3C)	F 5'- TCCCTCCAAGGTAAGAGCCCG -3' R 5'- AGGGACAAACTTGGCAGCAGTC -3'	Eurogentec[1]
F14 (3C)	F 5'- CTGCATGGGCAGACAAGGACC -3' R 5'- CAGGCAGCCACTACTACAGAAG -3'	Eurogentec[1]
F33 (3C)	F 5'- GCTCAACGAAGAGATCAGGCAC -3' R 5'- GCATCCATCCAGGCTACGCTTC -3'	Eurogentec[1]
F16 (DLK1-WRE. 3C)	5'- CTCCCTCCACGGCTCAGATC-3'	Eurogentec[1]
F4 (3C)	5'-GGCAGGTATAGCATCATACTCCC-3'	Eurogentec[1]
F5 (3C)	5'-CATGTCCCATGTGGCCACTTGC-3'	Eurogentec[1]
F10 (3C)	5'-CTATCTCCAAGTGGTCTTGGCC-3'	Eurogentec[1]
F11 (3C)	5'-GATGAGCGTGGCACTCAGACC-3'	Eurogentec[1]
F12 (3C)	5'-CCACATCTGGCCAGTGCTTGC-3'	Eurogentec[1]
F17 (3C)	5'-CTTGGTTCACCCATCCTTGGCC-3'	Eurogentec[1]
F20 (3C)	5'-GCAGTAGTAGCACCTGCTGGTC-3'	Eurogentec[1]
F21 (3C)	5'-GCTCAGAGCTGGAGAGACAGAC-3'	Eurogentec[1]
F22 (3C)	5'-CCATGCTATTGGAGGTCCTGGG-3'	Eurogentec[1]
F23 (3C)	5'-CCTGGGTGCCCCCAAAATACAC-3'	Eurogentec[1]
F24 (3C)	5'-GTGGGCCATTTCTGCAGGGTG-3'	Eurogentec[1]
F31 (3C)	5'-CAGCACTCGGTTCTGCTACCAG-3'	Eurogentec[1]
F32 (3C)	5'-GACCAAGGGTTTCATGGGGCAG-3'	Eurogentec[1]
F34 (3C)	5'-CTGCTGCAAGGTTTGGAGGATG-3'	Eurogentec[1]
Meg3 (in situ hybridization)	Sens: 5'AAGAAGACTGAGGACCCCAGGA-3' Antisens 5'-TGTGTCCGTGTGTCCAGGGT-3'	Eurogentec[1]
miR-127 probe (in situ hybridization)	MIMAT0004604	Exiqon/ Thermo Fisher[2]
Hsa-miR-127	000452	Thermo Fisher[2]
sno135	001230	Thermo Fisher[2]
Meg3 mouse	Mm00522599	Thermo Fisher[2]
MEG3 human	Hs00292028	Thermo Fisher[2]
Glul mouse	Mm00725701	Thermo Fisher[2]
GLUL human	Hs00365928_g1	Thermo Fisher[2]
Apc total form	Mm00545877	Thermo Fisher[2]
Apc deleted form	Mm01130462	Thermo Fisher[2]
human RIAN (MEG8)	Hs00419701_m1	Thermo Fisher[2]
human MIRG (MEG9)	Hs01593046_s1	Thermo Fisher[2]
mouse Rian	Mm01325842_g1	Thermo Fisher[2]
mouse Mirg	Mm01335848	Thermo Fisher[2]
human RTL-1	Hs06637009_s1	Thermo Fisher[2]
mouse Rtl-1	Mm02392620_s1	Thermo Fisher[2]
DLK1-WRE (ChIP)	ART2AUJ	Thermo Fisher[2]
Afp-220kb (ChIP control)	AJHSN1G	Thermo Fisher[2]

Table S10: lists of antibodies and kits used

WB: western-blot. IHC: Immunohistochemistry

| Name	Supplier	Reference	Quantity/Dilution
Glutamine synthétase	BD Biosciences, Franklin Lakes, NJ	610518	1/400 (IHC)
Ki67	Abcam, Cambridge, UK	Ab16667	1/300 (IHC)
Cleaved Caspase 3	Cell Signaling, Danvers, MA	#9661	1/600 (IHC)
DLK1	Proteintech, San Diego, CA	10636-1-AP	1/1000 (WB)
Cyclin A2	Abcam, Cambridge, UK	ab 32386	1/100 (WB)
Cyclin B1	Cell Signaling, Danvers, MA	4138	1/200 (WB)
FOXM1	Santa Cruz Biotechnology, Dallas, TX	sc-376471 X	10ug (CHIP) , 1/100 (IHC)
CD45 -PE	BD Biosciences, Franklin Lakes, NJ	553081	1/400 (flow cytometry)
CD31 – BV605	BioLegend, San Diego, CA	102427	1/300 (flow cytometry)
CD11b – BV510	BD Biosciences, Franklin Lakes, NJ	562950	1/400 (flow cytometry)
CD11c – PE Cy.7	BD Biosciences, Franklin Lakes, NJ	558079	1/400 (flow cytometry)
F4/80 – Percp Cy 5.5	Thermofischer, Waltham, MA	130-118-466	1/300 (flow cytometry)
Ly6C – V450	BD Biosciences, Franklin Lakes, NJ	560594	1/200 (flow cytometry)
Ly6G – APC Cy.7	BioLegend, San Diego, CA	127624	1/200 (flow cytometry)
TCF-4	Millipore, Burlington, MA	05-511	3ug (CHIP)
β-catenin	BD Biosciences Franklin Lakes, NJ	610154	1/50 (IHC), 10µg (CHIP)
HNF-4α	Santa-Cruz, Dallas, TX	sc-6556x	10µg (CHIP)
H3K27ac	Active Motif, Carlsbad, CA	39133	10µg (CHIP)
H3K4me3	Active Motif, Carlsbad, CA	39159	5 µg (CHIP)
H3K4me1	Active Motif, Carlsbad, CA	39297	10µg (CHIP)
β-actin	Sigma-Aldrich, Saint-Louis, CA	A5441	1/5000 (WB)
FADD	Elabscience, Houston, TX	E-AB-10318	1/1000 (WB)
mouse on mouse kit	Vector Lab, Newark, CA	BMK2202	
Anti-rabbit biotinylated	Vector Lab, Newark, CA	BA-1000	1/200 (IHC)
Histofine kit	Microm Microtech, Brignais, France	F/414341F	
Anti-rabbit HRP	Cell Signaling, Danvers, MA	7074	1/2000 (WB)
Anti-mouse HRP	Cell Signaling, Danvers, MA	7076	1/2000 (WB)
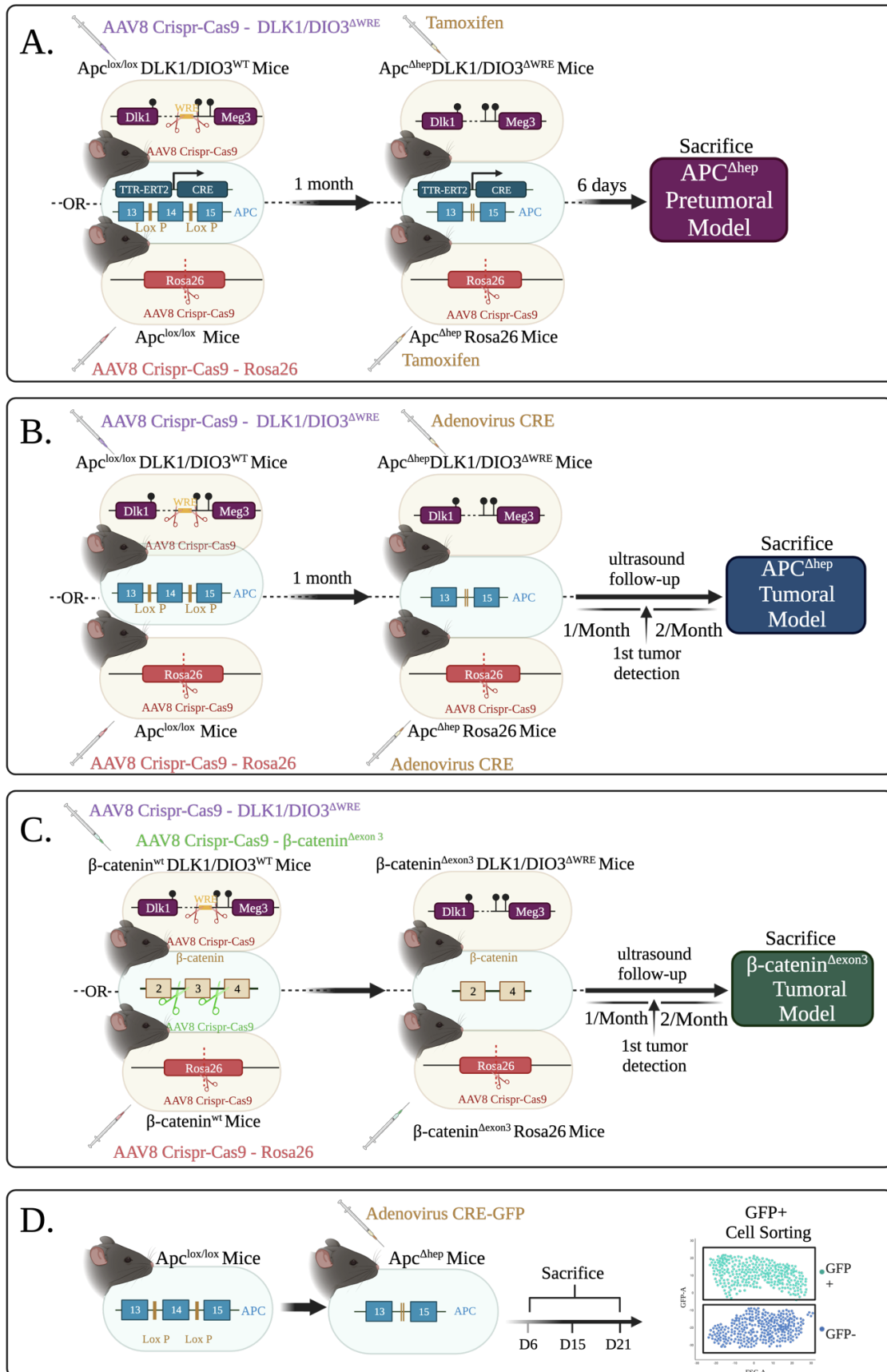
Figure S1: Schematic representation of experimental models

A-B: Generation of Apc$^{\Delta hep}$-DLK1/DIO3$^{\Delta WRE}$ model with AAV8 CRISPR/Cas9 constructs targeting the DLK1-WRE site in Apc$^{lox/lox}$ model: tamoxifen-induced *Apc* deletion was conducted one month after AAV8 injection, which is the time that we have identified as optimal for gene editing[2] in pretumoral model (**A**) and tumoral model (**B**); **C:** Generation of β-catenin$^{\Delta Exon3}$ DLK1/DIO3$^{\Delta WRE}$ model with concomitant injection of AAV8 CRISPR/Cas9 constructs targeting *Ctnnb1* and the DLK1-WRE site; **D:** Kinetics of hepatocyte sorting: GFP-positive hepatocytes were sorted from tumoral Apc$^{\Delta hep}$ livers in early-steps by flow cytometry (ARIA3, BD). GFP- and GFP+ hepatocytes from Apc$^{wt/wt}$ mice were used as control hepatocytes. Figure made with Biorender.
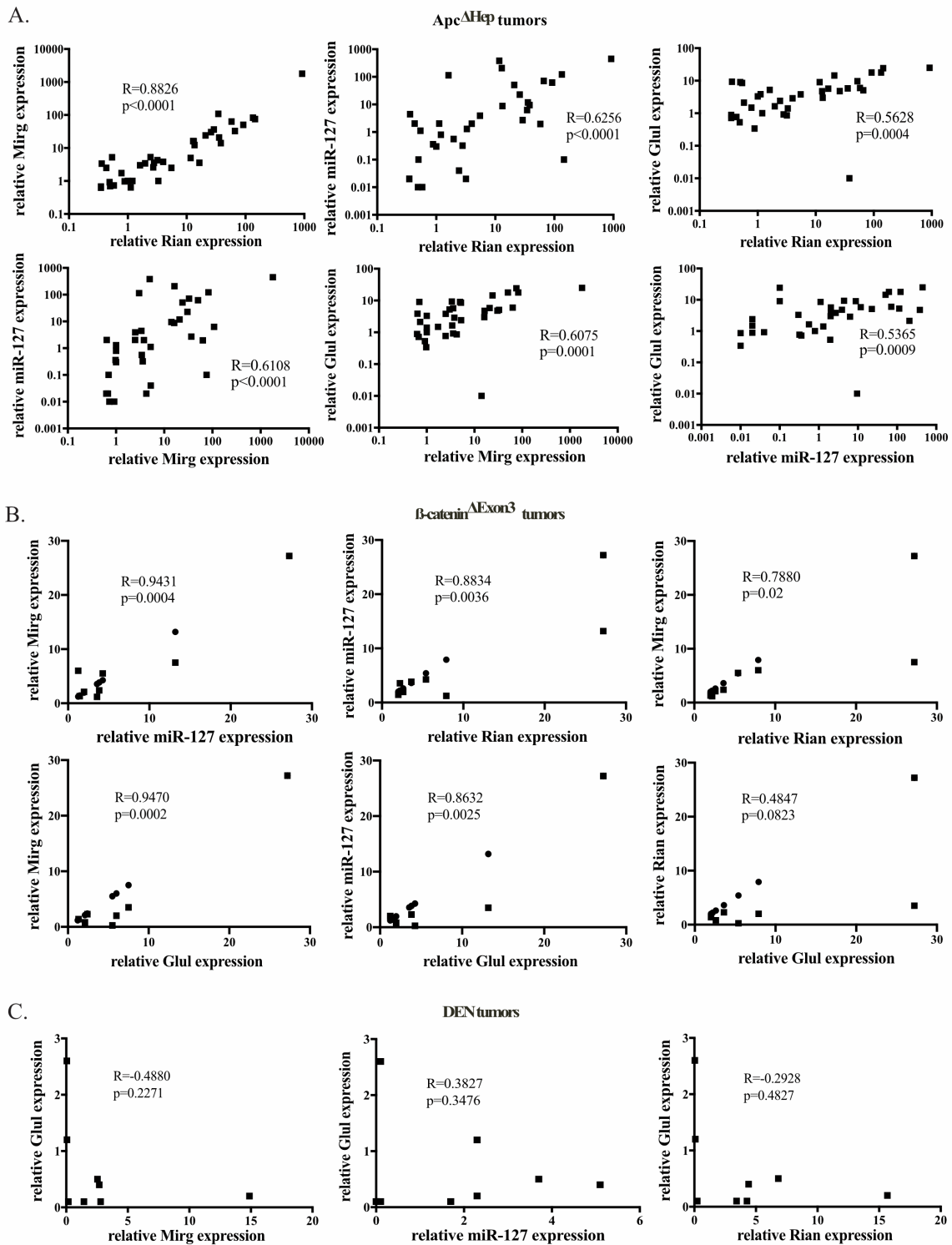
Figure S2

Figure S2: Correlation between expression levels of RNAs within the *Dlk1/Dio3* locus and *Glul* in Apc$^{\Delta hep}$, β-catenin$^{\Delta Exon3}$ and DEN tumors

A-C: Correlation between *Rian*, *Mirg*, miR-127, and *Glul* expression levels by RT-qPCR in Apc$^{\Delta hep}$ tumors (**A**), β-catenin$^{\Delta Exon3}$ tumors (**B**), and DEN tumors (**C**).
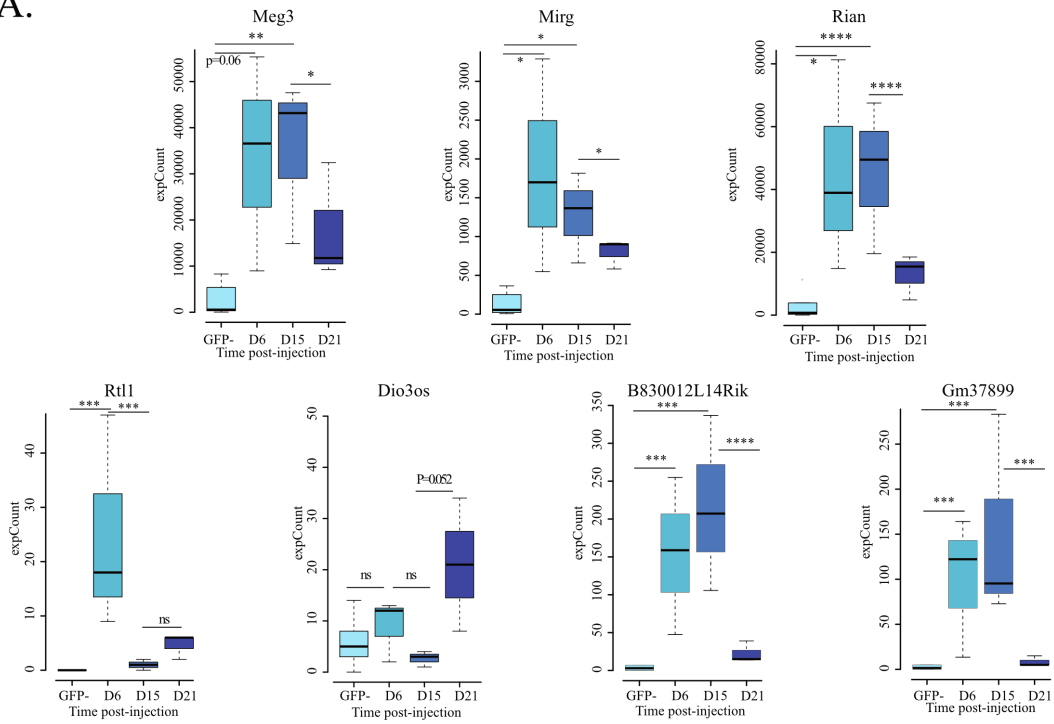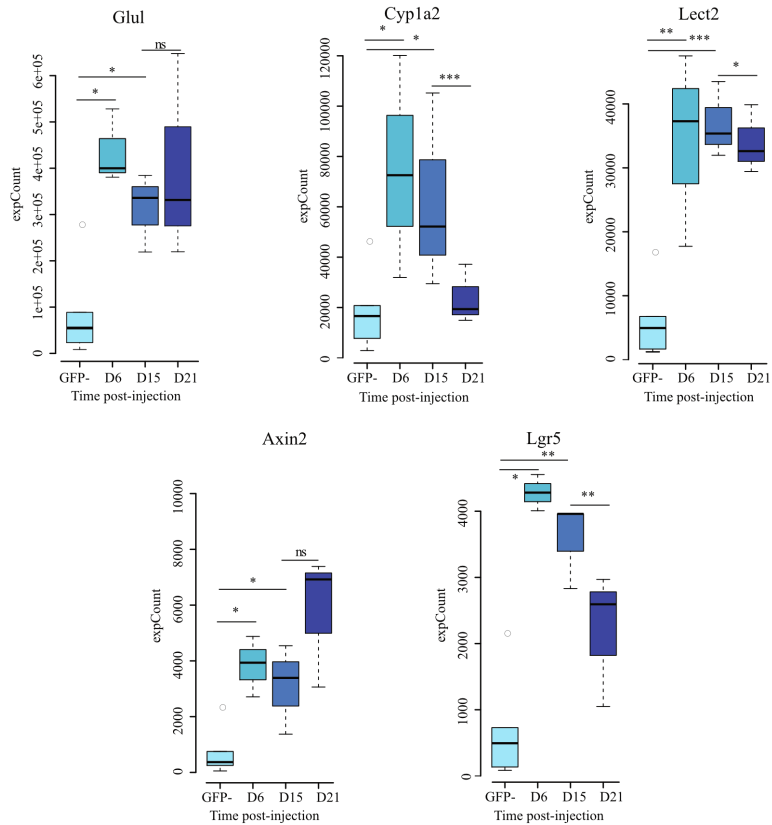
Figure S3

Figure S3: RNAs within the *Dlk1/Dio3* locus are induced during the earliest phases of tumorigenesis in Apc$^{\Delta hep}$ model

A-B: RNA-seq data analyses from sorted hepatocytes at day 6, 15 and day 21 after injection of an adenovirus Cre-GFP and subsequent activation of β-catenin signaling in Apc$^{\Delta hep}$ model. Box plots represent the mean normalized RPKM of at least three independent samples; **A:** RNAs from the *DLK1/DIO3* locus; **B:** canonical target genes of β-catenin. Levels of significance: *p<0.05, ** p<0.01, ***p<0.005, ****p<0.0001, ns: non-significant (Mann-Whitney), with error bars representing s.e.m..

.
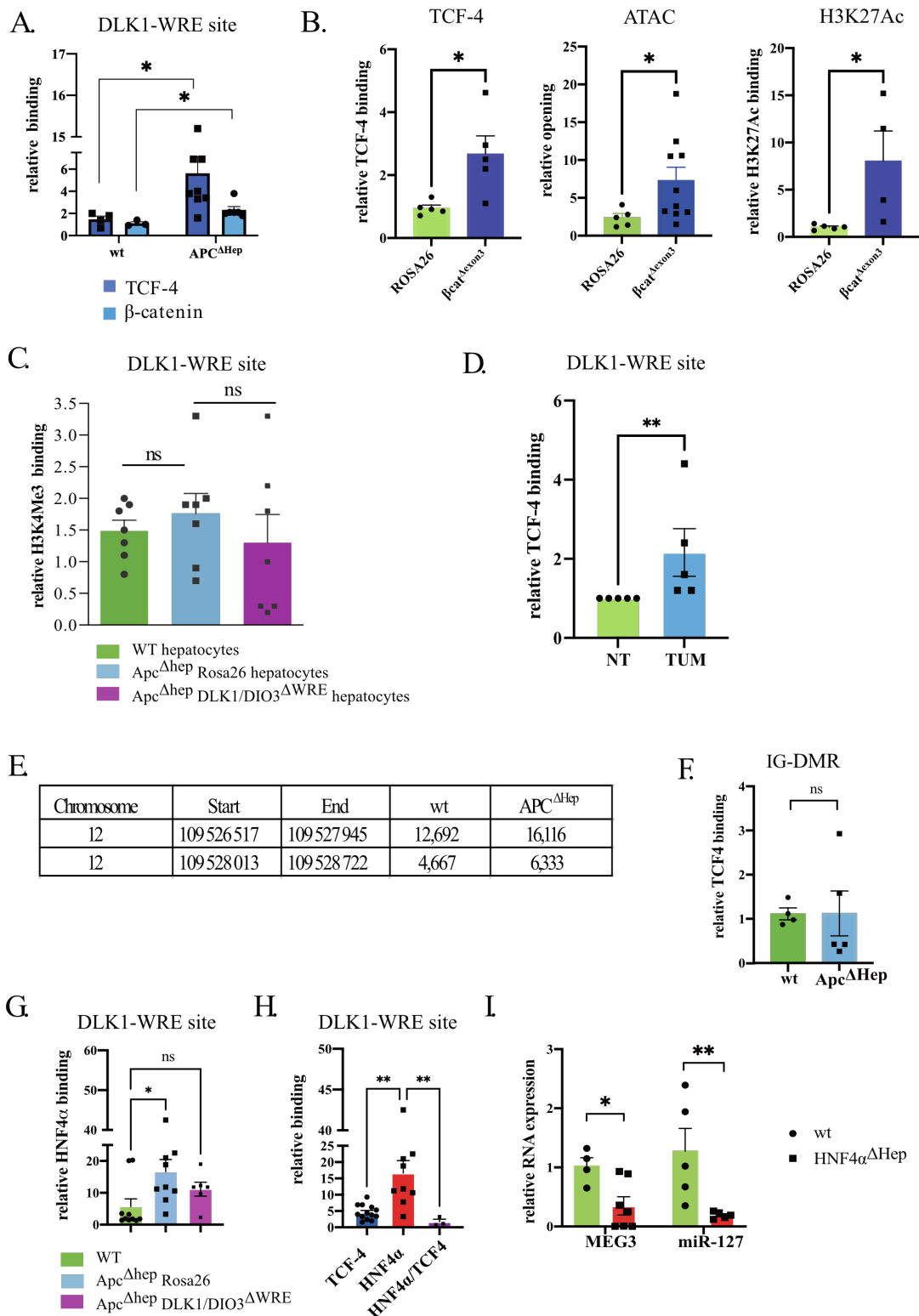
Figure S4

Figure S4: ChIP- and ATAC-qPCR validations

A: ChIP-qPCR analysis of β-catenin and TCF-4 binding at the DLK1-WRE site in wild-type (wt) and Apc$^{\Delta hep}$ hepatocytes relative to isotype control; **B:** ChIP-qPCR analysis of TCF-4 and H3K27ac relative binding to isotype control and ATAC-qPCR performed in Rosa26 (green) and β-catenin$^{\Delta Exon3}$ hepatocytes (blue); **C:** ChIP-qPCR analysis of H3K4me3 marks at DLK1-WRE site in wt, Apc$^{\Delta hep}$-Rosa26 and Apc$^{\Delta hep}$-DLK1/DIO3$^{\Delta WRE}$ hepatocytes binding to isotype control; **D:** ChIP-qPCR analysis of TCF-4 binding at the DLK1-WRE site in Apc$^{\Delta hep}$ and β-catenin$^{\Delta Exon3}$ tumors (TUM) compared to isotype control and adjacent non-tumor tissues (NT); **E:** methylation status of IG-DMR obtained by MeDIP-seq (GSE239777) in Apc$^{\Delta hep}$ *versus* wild-type hepatocytes; **F:** ChIP-qPCR analysis of TCF-4 binding at the IG-DMR site in Apc$^{\Delta hep}$ *versus* wt hepatocytes relative to isotype control; **G**: HNF4α binding at the DLK1-WRE site in wt, Apc$^{\Delta hep}$-Rosa26 and Apc$^{\Delta hep}$-DLK1/DIO3$^{\Delta WRE}$ hepatocytes relative to isotype control; **H:** sequential ChIP-qPCR analysis for HNF4α and TCF-4 at the DLK1-WRE site in Apc$^{\Delta hep}$-Rosa26 hepatocytes relative to isotype control; **I:** *Meg3* and miR-127 expression determined by RT-qPCR in HNF4α$^{\Delta hep}$ hepatocytes. Levels of significance: *p<0.05, ** p<0.01, ns: non-significant (Mann-Whitney or Kruskal-Wallis), with error bars representing s.e.m..
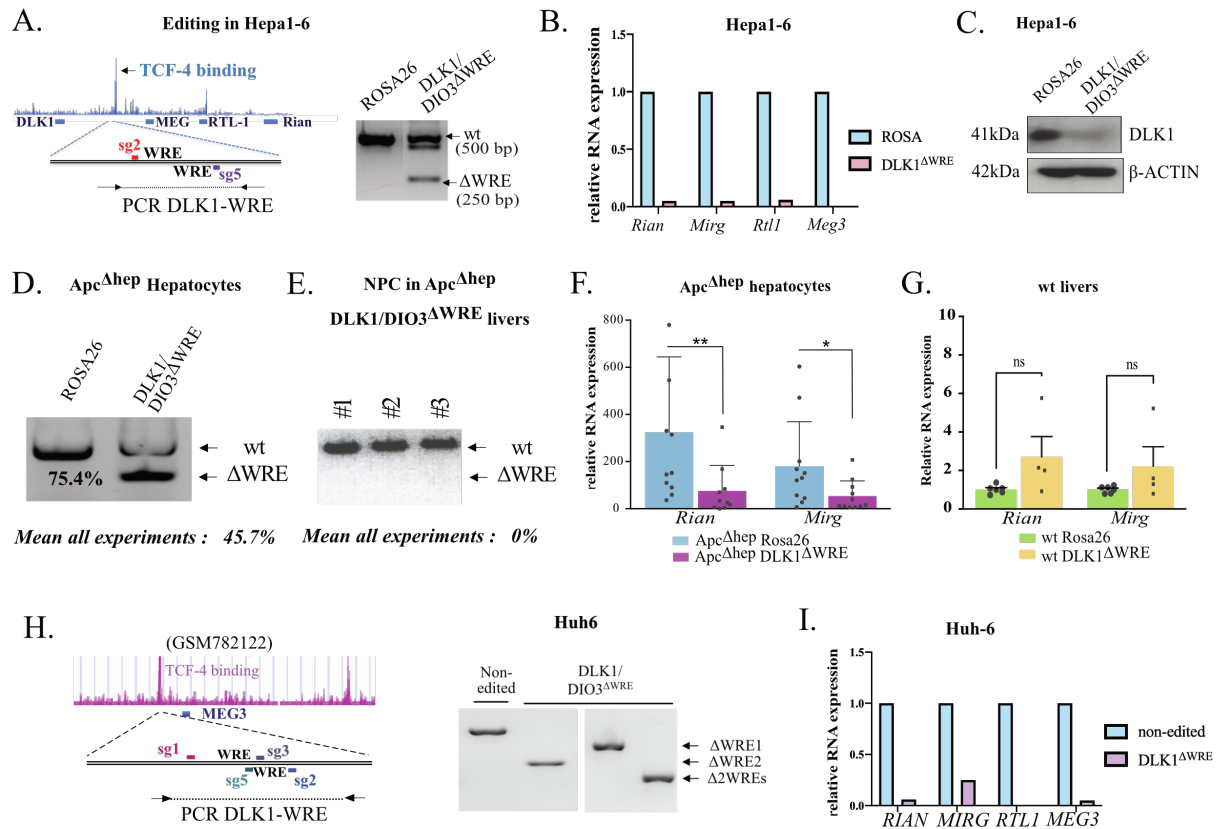
Figure S5

Figure S5: Validation of CRISPR/Cas9 constructs in hepatic cancer cell lines and in Apc$^{\Delta hep}$ livers *in vivo*

A: Design of 2 sgRNAs to delete the TCF-4 binding site upstream of *Meg3* (left panel) and representative PCR analysis of the DLK1-WRE region showing the deleted band (ΔWRE) and the full band (WT) (right panel) in Hepa1-6 clones; **B:** *Rian, Mirg, Meg3,* and *Rtl1* expression determined by RT-qPCR in DLK1/DIO3$^{\Delta WRE}$ Hepa1-6 clones compared to Rosa26 controls; **C:** DLK1 protein level determined by Western-blot in Hepa1-6 clones; **D:** Efficiency of CRISPR/Cas9 editing by AAV8 injection *in vivo* on isolated Apc$^{\Delta hep}$-Rosa26 and Apc$^{\Delta hep}$-DLK1/DIO3$^{\Delta WRE}$ hepatocytes. A representative PCR analysis of the DLK1-WRE region is shown with quantification of the deleted band with ImageJ as well as the mean of all experiments indicated below **E:** representative PCR analysis of the DLK1-WRE region showing no deleted band on three samples of non-parenchymal cells (NPCs) isolated from Apc$^{\Delta hep}$-DLK1/DIO3$^{\Delta WRE}$ livers; **F-G:** Relative expression of *Rian* and *Mirg* by RT-qPCR in isolated Apc$^{\Delta hep}$-DLK1/DIO3$^{\Delta WRE}$ *versus* Apc$^{\Delta hep}$-Rosa26 hepatocytes compared to wild-type hepatocytes (**F**) and in wt-DLK1/DIO3$^{\Delta WRE}$ livers compared to wt-Rosa26 livers (**G**); **H:**

Design of 4 sgRNAs to delete the TCF-4 binding site upstream of *MEG3*, which contains 2 WREs identified from the publicly available ChIP-seq data targeting TCF-4 in the human hepatoblastoma HepG2 cell line (Gsm782122) (left panel); representative PCR analysis showing the deleted band (ΔWRE) in DLK1/DIO3$^{\Delta WRE}$ Huh6 clones for three couples of sgRNAs deleting one or both WREs (right panel); the two PCR images show all types of clones emerging in a 96-well plate and thus originate from distinct regions of the same gel of screening; **I:** *MEG3*, *MIRG*, *RTL-1,* and *RIAN* expression by RT-qPCR in DLK1/DIO3$^{\Delta WRE}$ Huh6 clones compared to non-edited Huh6 control clones. Levels of significance: *p<0.05, ** p<0.01, ns: non-significant (Mann-Whitney), with error bars representing s.e.m..
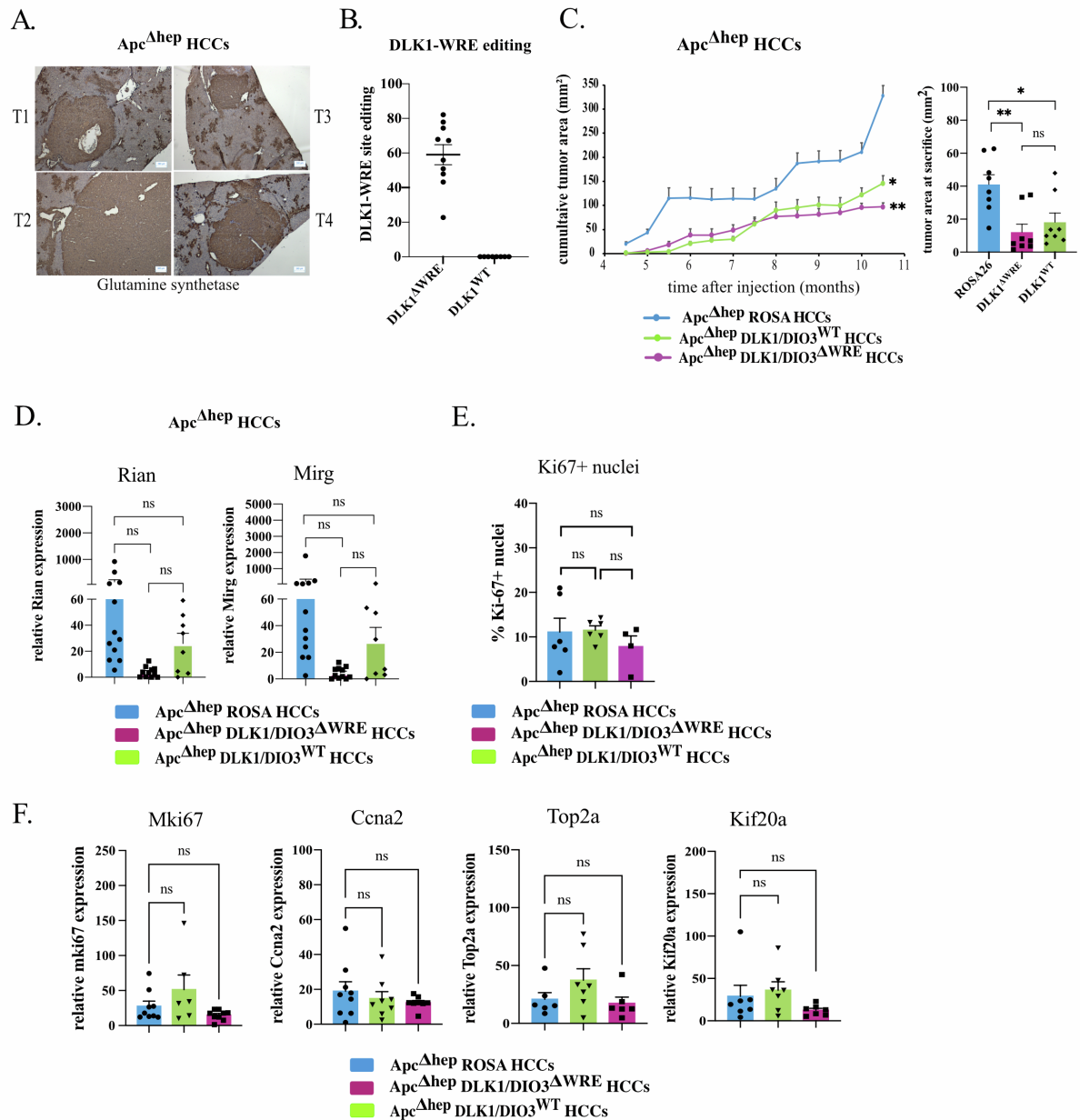
Figure S6

Figure S6: DLK1-WRE site editing slows Apc$^{\Delta hep}$ HCC growth but does not affect the expression of the identified actors involved in G2/M phase

A: Examples of glutamine synthetase staining of Apc$^{\Delta hep}$ HCCs; **B:** analysis of tumor editing by PCR band quantification with ImageJ in Apc$^{\Delta hep}$ HCC; **C:** Progression of cumulative tumor areas (left panel) and areas at sacrifice (right panel) for Apc$^{\Delta hep}$ HCC; **D:** RT-qPCR analysis of *Rian* and *Mirg* expression in Apc$^{\Delta hep}$ HCC compared to their adjacent non-tumor tissues; **E:** Percentage of Ki-67+ hepatocytes in Apc$^{\Delta hep}$ HCC; **F:** Expression of *Mki67*, *Ccna2*, *Top2a*, and

Kif20a determined by RT-qPCR relative to their adjacent non-tumor tissues in Apc$^{\Delta hep}$ HCC. Levels of significance: *$p<0.05$, ** $p<0.01$, ns: non-significant (Kruskal-Wallis), with error bars representing s.e.m..
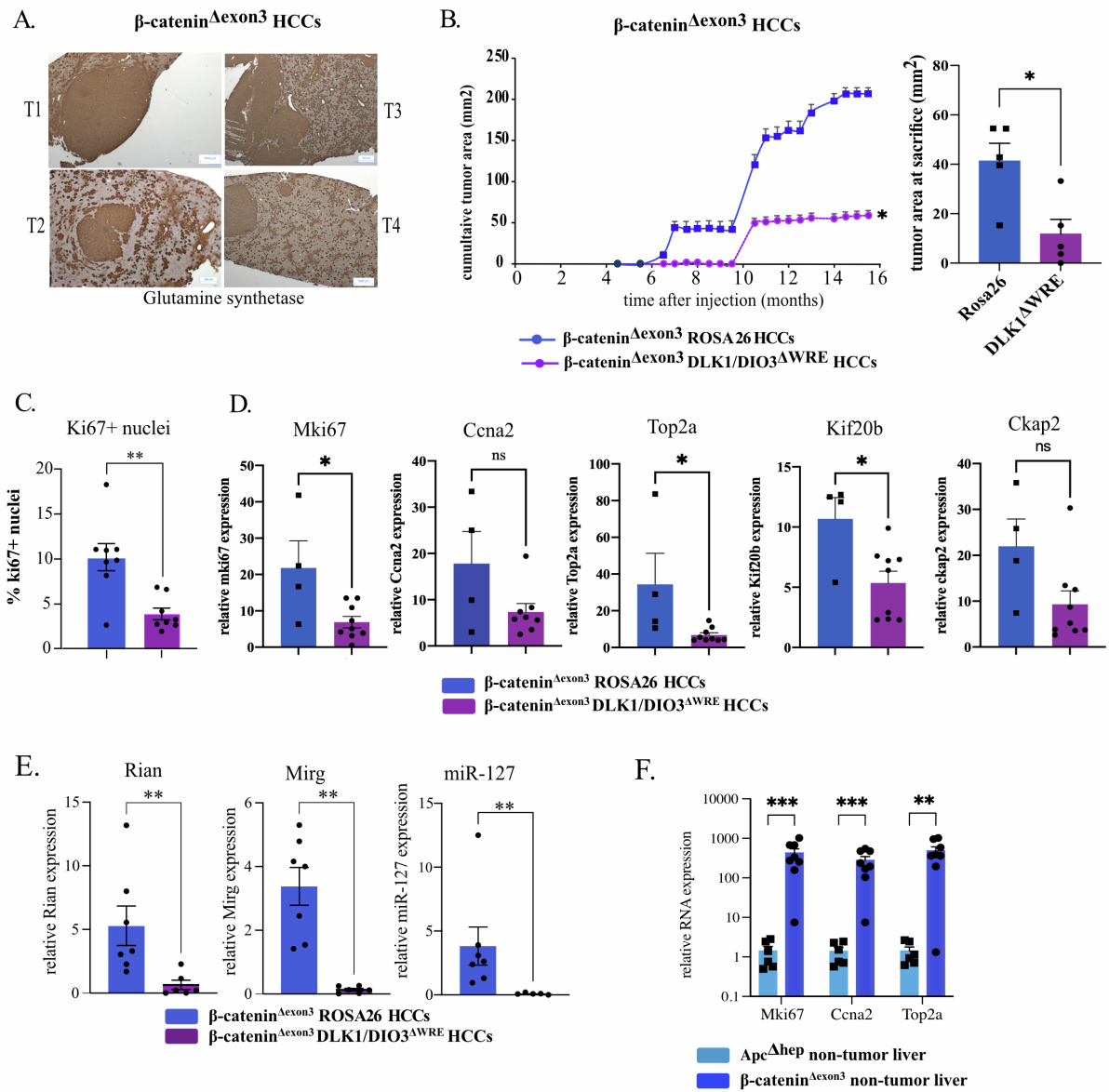
Figure S7

Figure S7: DLK1-WRE site editing slows β-catenin$^{\Delta Exon3}$ HCC growth

A: Examples of glutamine synthetase staining of β-catenin$^{\Delta Exon3}$ HCC; **B**: Progression of cumulative tumor areas (left panel) and areas at sacrifice (right panel) for β-catenin$^{\Delta Exon3}$ HCC; **C:** Percentage of Ki-67+ hepatocytes in β-catenin$^{\Delta Exon3}$ HCC; **D:** Expression of *Mki67*, *Ccna2*, *Top2a*, *Kif20b,* and *Ckap2* determined by RT-qPCR in β-catenin$^{\Delta Exon3}$ HCC relative to their adjacent non-tumor tissues; **E:** RT-qPCR analysis of *Rian*, *Mirg* and miR-127 in β-catenin$^{\Delta Exon3}$ HCC compared to their adjacent non-tumor tissues; **F:** RT-qPCR analysis of *Mki67*, *Ccna2* and *Top2a* in Apc$^{\Delta hep}$ and β-catenin$^{\Delta Exon3}$ non-tumor tissues. Levels of significance: *p<0.05,

**p<0.01, *** p<0.005, ns: non-significant (Mann-Whitney), with error bars representing s.e.m..

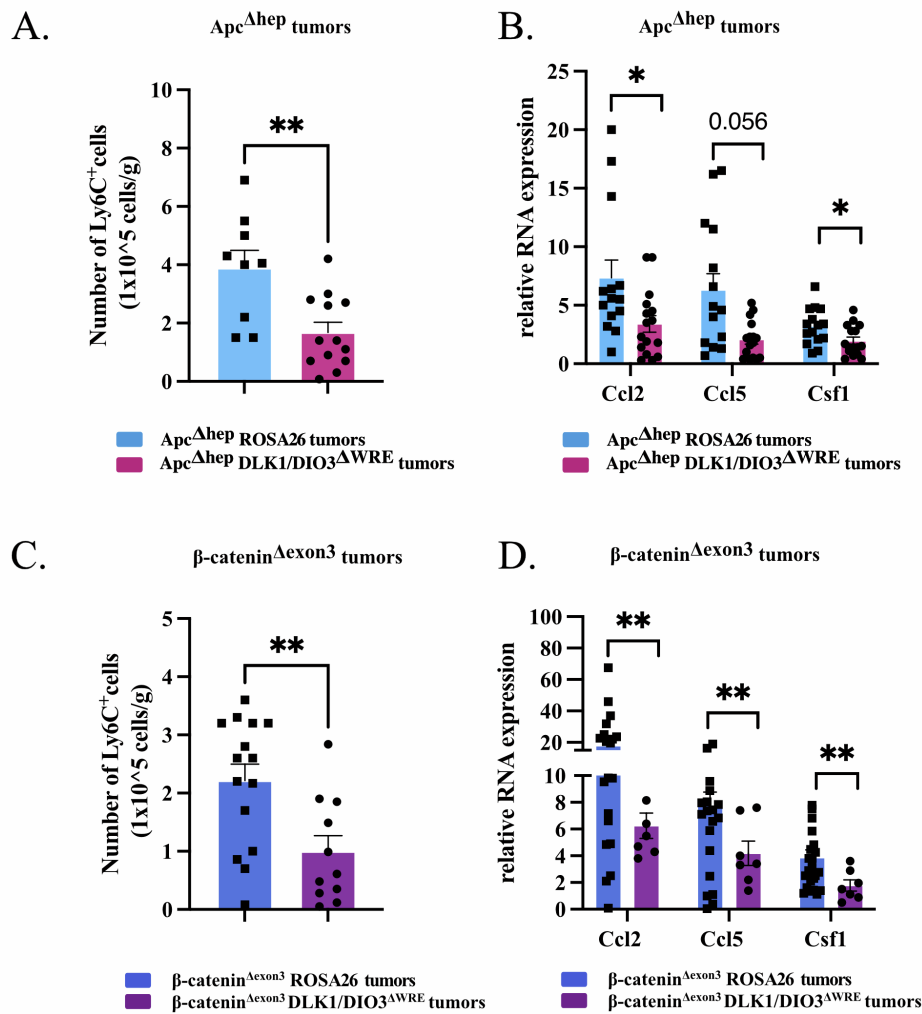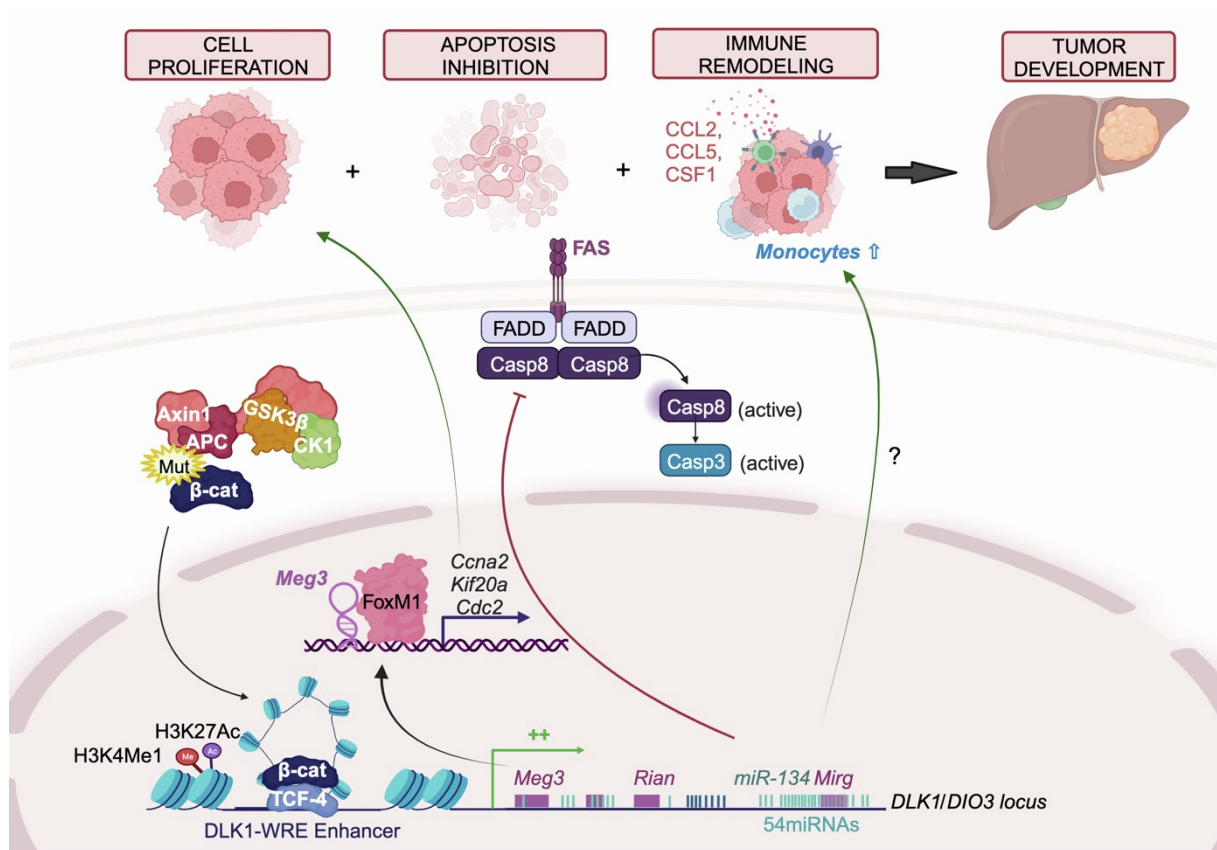**Figure S8**

Figure S8: DLK1-WRE site editing impairs monocyte recruitment in Apc$^{\Delta hep}$ and β-catenin$^{\Delta Exon3}$ tumors.

A, C: Absolute number of Ly6C+ monocytes relative to tissue weight in Apc$^{\Delta hep}$ (**A**) and β-catenin$^{\Delta Exon3}$ tumors (**C**); **B, D:** RT-qPCR analysis of *Ccl2*, *Ccl5*, and *Csf1* relative to their adjacent non-tumor tissues in Apc$^{\Delta hep}$ tumors (**B**) and β-catenin$^{\Delta Exon3}$ tumors (**D**). Levels of significance: *p<0.05, ** p<0.01 (Mann-Whitney), with error bars representing s.e.m..

Figure S9: Graphical abstract

Figure made with Biorender.

References:

1. Hirsch, T. Z., Pilet, J., Morcrette, G., Roehrig, A., Monteiro, B. J. E., Molina, L., Bayard, Q., Trepo, E., Meunier, L., Caruso, S. *et al.* Integrated Genomic Analysis Identifies Driver Genes and Cisplatin-Resistant Progenitor Phenotype in Pediatric Liver Cancer. (2021). Cancer Discov. 11, 2524-2543, doi:10.1158/2159-8290.CD-20-1809
2. Loesch, R., Caruso, S., Paradis, V., Godard, C., Gougelet, A., Renault, G., Picard, S., Tanaka, I., Renoux-Martin, Y., Perret, C. *et al.* Deleting the beta-catenin degradation domain in mouse hepatocytes drives hepatocellular carcinoma or hepatoblastoma-like tumor growth. (2022). J Hepatol. doi:10.1016/j.jhep.2022.02.023